

## Band structure and Fermi surface of URu<sub>2</sub>Si<sub>2</sub> studied by high-resolution angle-resolved photoemission spectroscopy

T. Ito, H. Kumigashira, and T. Takahashi

*Department of Physics, Tohoku University, Sendai 980-8578, Japan*

Y. Haga, E. Yamamoto, and T. Honma

*Advanced Science Research Center, Japan Atomic Energy Research Institute, Tokai, Ibaraki 319-1195, Japan*

H. Ohkuni

*Department of Physics, Osaka University, Toyonaka 560-0043, Japan*

Y. Ōnuki

*Department of Physics, Osaka University, Toyonaka 560-0043, Japan*

*and Advanced Science Research Center, Japan Atomic Energy Research Institute, Tokai, Ibaraki 319-1195, Japan*

(Received 22 February 1999)

We have performed a high-resolution angle-resolved photoemission spectroscopy (ARPES) on single-crystal URu<sub>2</sub>Si<sub>2</sub> to study the band structure and the Fermi surface in the paramagnetic phase. The valence-band structure consisting of the Ru 4*d* and Si 3*p* states shows a qualitatively good agreement between the ARPES experiment and the band-structure calculation. In the vicinity of the Fermi level ( $E_F$ ), we observed a less dispersive band, which crosses  $E_F$  midway between the Z and X points in the Brillouin zone. Comparison with the band calculation as well as with the de Haas–van Alphen (dHvA) result suggests that the experimental band near  $E_F$  is assigned to the largest hole pocket centered at the Z point, which has a strong U 5*f*-Ru 4*d* hybridized character. The observed remarkable narrowing of the near- $E_F$  band compared with the band-structure calculation suggests a strong renormalization effect due to the electron correlation of U 5*f* electrons. [S0163-1829(99)01343-0]

### I. INTRODUCTION

The heavy fermion superconductor URu<sub>2</sub>Si<sub>2</sub> has attracted much attention because of its anomalous physical properties as represented by the coexistence of the antiferromagnetic ordering ( $T_N=17.5$  K) and the superconductivity ( $T_c=1.5$  K).<sup>1–5</sup> The electronic specific heat coefficient ( $\gamma$ ) shows a drastic change at  $T_N$  from  $\gamma=180$  to 50 mJ/mol K<sup>2</sup> (Ref. 6), suggesting the development of a charge- or a spin-density wave below  $T_N$  (Ref. 2). The complicated electronic and magnetic properties of URu<sub>2</sub>Si<sub>2</sub> at low temperatures have been regarded to originate in the fundamental character of U 5*f* electrons.<sup>5</sup> The U 5*f* states located near the Fermi level ( $E_F$ ) are expected to strongly hybridize with the Ru 4*d* orbital near  $E_F$  and produce the complicated Fermi surface(s), leading to the various electronic and magnetic orderings at low temperatures. The Fermi surface of URu<sub>2</sub>Si<sub>2</sub> has been intensively studied by the de Haas-van Alphen (dHvA) effect measurements,<sup>7–9</sup> which have reported several independent oscillations ascribable to the Fermi surfaces in URu<sub>2</sub>Si<sub>2</sub>. However, the experimental results are not necessarily consistent with each other and it is hard at present to discuss the Fermi-surface topology in detail. An alternative information from a different experimental technique has been required.

Angle-resolved photoemission spectroscopy (ARPES) is a unique and powerful experimental technique to study the electronic band structure of materials.<sup>10</sup> ARPES has been employed on various materials and successfully established the valence-band structure. However, the energy resolution

was not necessarily enough to discuss the detailed electronic structure near  $E_F$ , in particular for the so-called *f*-electron materials where 4*f* or 5*f* electrons produce the complicated narrow “bands” near  $E_F$ . A recent remarkable improvement in the energy and angular resolutions in ARPES has enabled the precise probing of the momentum-resolved electronic structure near  $E_F$ . Using high-resolution (HR) ARPES, we have studied the detailed band structure near  $E_F$  of some 4*f*- and 5*f*-electron materials such as CeSb (Ref. 11) and UPt<sub>3</sub> (Ref. 12) and demonstrated the high capability of HR-ARPES to study the Fermi-surface topology and its evolution as a function of temperature.

In this paper, we report the result of our HR-ARPES study on URu<sub>2</sub>Si<sub>2</sub>. We have successfully determined the whole valence-band structure consisting of mainly the Ru 4*d* and Si 3*p* states. The result shows a good qualitative agreement with the band-structure calculation. Beside the highly dispersive Ru 4*d* and Si 3*p* bands, we also found a less dispersive narrow band near  $E_F$ , which crosses  $E_F$  midway between two high-symmetry points in the Brillouin zone and forms a large Fermi surface. We compare the present ARPES result with the band-structure calculation as well as with the dHvA to discuss the Fermi-surface topology and the renormalization effect due to the strong electron correlation in the band structure.

### II. EXPERIMENT

URu<sub>2</sub>Si<sub>2</sub> single crystals (typically 3–4 mm in diameter and 80 mm in length) were grown by the Czochralski method with a tetra-arc furnace. The starting materials were

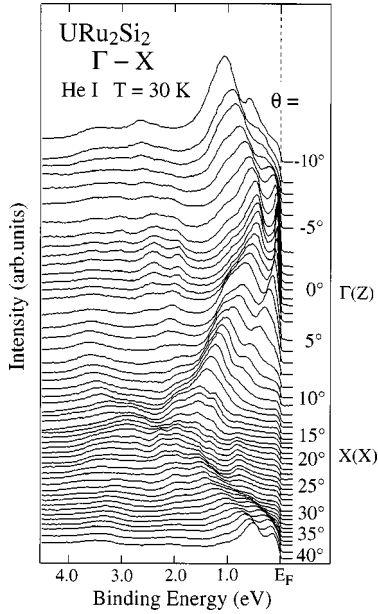


FIG. 1. ARPES spectra of URu<sub>2</sub>Si<sub>2</sub> measured at 30 K (paramagnetic phase) with He I resonance line (21.2 eV) in the  $\Gamma$ X- $X$ RZ plane in the Brillouin zone. Polar angle ( $\theta$ ) with respect to the surface normal is indicated.

99.95% pure U, 99.99% pure (4N) Ru and 5N Si. The obtained crystals were annealed at 900 °C for a week under vacuum and then characterized by x-ray diffraction to confirm the single crystallinity.

Photoemission measurement was carried out using a home-built high-resolution photoemission spectrometer, which has a hemispherical electron energy analyzer and a highly bright discharge lamp. The base pressure of the spectrometer is  $3 \times 10^{-11}$  torr and the angular resolution is  $\pm 1^\circ$ . The energy resolution was set at 30–50 meV for quick data acquisition because of the relatively fast degradation of sample surface. A clean mirrorlike surface of URu<sub>2</sub>Si<sub>2</sub> (001)

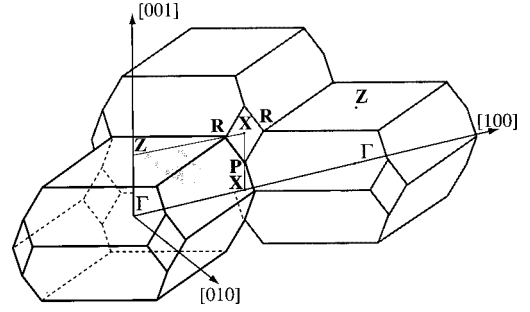


FIG. 2. Brillouin zone of URu<sub>2</sub>Si<sub>2</sub> with a body-centered tetragonal crystal structure. ARPES measurement was performed in the  $\Gamma$ X- $X$ RZ plane.

plane was obtained by *in situ* cleaving at 30 K just before measurement and kept at the same temperature during the measurement. Since we observed degradation of the sample surface as evident by the gradual increase of background in the spectrum, we recorded all the spectra within twenty hours after cleaving. We have checked that the spectral feature was unchanged within this time interval. We measured three sets of ARPES spectra using different samples and confirmed the reproducibility. The Fermi level of the samples was referred to that of a gold film evaporated on the sample substrate and its accuracy is estimated to be less than 5 meV.

### III. RESULTS AND DISCUSSION

Figure 1 shows a set of ARPES spectra of URu<sub>2</sub>Si<sub>2</sub> measured with the He I resonance line (21.2 eV) at 30 K for the  $\Gamma$ X- $X$ RZ plane in the body-centered tetragonal Brillouin zone (Fig. 2). Polar angle  $\theta$  measured from the surface normal of the cleaved (001) plane is denoted on spectra. We find that the position and intensity of structures in ARPES spectra are very sensitive to the polar angle. For example, we find several prominent peaks (bands) located near  $E_F$  around  $\theta = 0^\circ$ , which show a remarkable energy dispersion toward

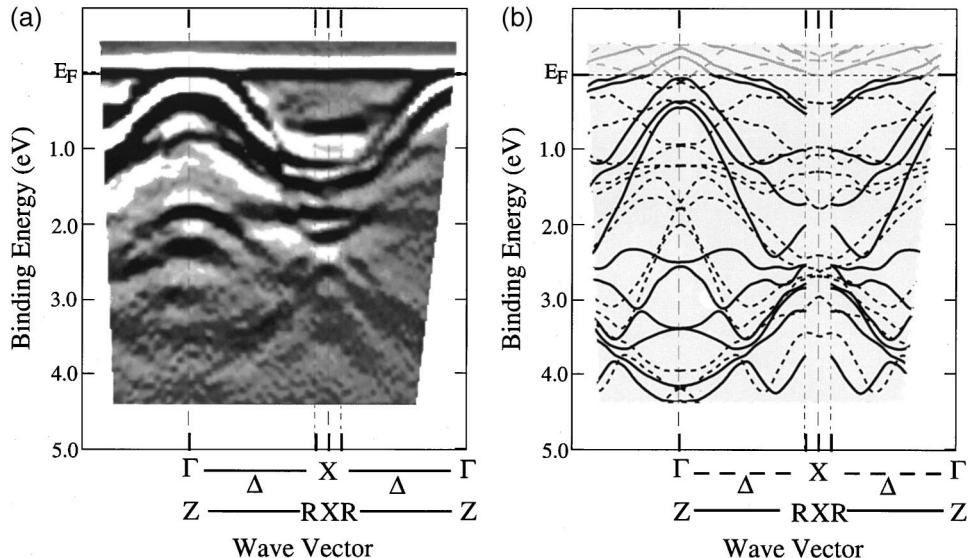


FIG. 3. Comparison of the valence-band structure of URu<sub>2</sub>Si<sub>2</sub> between (a) the ARPES experiment and (b) the band calculation (Ref. 16). The band-structure calculation has not presented the result between R and X points. Note the qualitatively good agreement in the band dispersions between the experiment and the calculation.

the higher binding energy with increasing or decreasing the polar angle. Since the polar angle of  $0^\circ$  corresponds to the high-symmetry point  $\Gamma(Z)$  in the Brillouin zone (see Fig. 2), we find that these bands show a symmetric dispersive feature with respect to the  $\Gamma(Z)$  point. These dispersive bands appear to have a bottom at 1.5–2 eV binding energy around  $\theta=22^\circ$ , which roughly corresponds to the Brillouin-zone boundary ( $X$  point). With further increasing the polar angle ( $\theta=30^\circ-40^\circ$ ), these bands again approach  $E_F$  as if the bands have a mirror symmetry with respect to  $\theta=22^\circ$ . This indicates that the bands enter the next Brillouin zone and the ARPES spectrum traces the band dispersions from the  $X(X)$  point to the  $\Gamma(Z)$  point in the next Brillouin zone (see Fig. 2). Thus, we find that the measured ARPES spectra follow well the periodicity of the bulk Brillouin zone and reflect the electronic structure of  $\text{URu}_2\text{Si}_2$ .

In order to see more directly the dispersive feature of bands as well as to compare it with the band-structure calculation, we have mapped out the ‘‘band structure’’ of  $\text{URu}_2\text{Si}_2$  from the ARPES spectra. The results are shown in Fig. 3(a) for the  $\Gamma X\text{-}XRZ$  plane. The experimental band structure has been obtained by taking the second derivative of ARPES spectra after moderate smoothing and plotting the intensity in a square-root scale by gradual shading as a function of the wave vector and the binding energy.<sup>10,13</sup> Using this numerical method, we can avoid artificial errors observed in a case of picking up the peak position by hand and also we can delete a background effect due to the spurious secondary electrons, which masks the real-energy position of peaks. In Fig. 3(a), dark areas correspond to the experimentally determined bands. We set the gray-scale level so as to have the apparent bandwidth in the gray-scale image being almost equal to the full width at half maximum of the corresponding peak in ARPES spectra.

Before comparing the experimental results with the calculation, we briefly explain what ‘‘band structure’’ the ARPES results correspond to. In the present experimental setup (see Fig. 2), we observe the electronic structure of the  $\Gamma X\text{-}XRZ$  plane in the Brillouin zone. In the photoemission process, the momentum of photoelectrons parallel to the surface is conserved owing to the existence of translational symmetry. In contrast, the above is not the case for the momentum perpendicular to the surface because of the surface potential. More importantly, the momentum itself has an uncertainty due to the very short escape depth of photoelectrons. Thus the momentum of photoelectron perpendicular to the surface becomes broad when the photoelectron escapes from the surface. This means that the ARPES spectrum reflects the electronic structure averaged out in the direction perpendicular to the surface ( $\Gamma Z$  direction in this case, see Fig. 2). As a result, the high-symmetry lines in the Brillouin zone are likely to appear as prominent structures in the ARPES spectrum because the density of states on the high-symmetry lines is relatively large. This indicates that the experimental band structure obtained by ARPES is compared with the band-structure calculation performed for the high-symmetry lines.<sup>13,14</sup> Of course, this interpretation is valid when the momentum broadening is comparable to or larger than the Brillouin zone (BZ) size in the perpendicular direction. The transition-matrix element and the final state effects may change the peak position in the spectrum.<sup>15</sup> Thus, it is noted

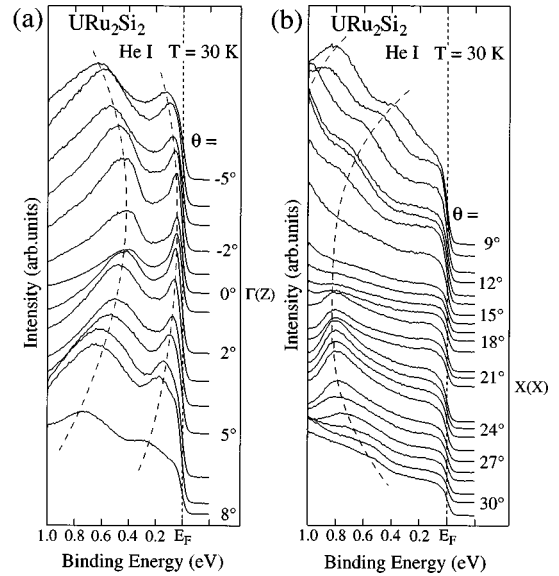


FIG. 4. ARPES spectra near  $E_F$  of  $\text{URu}_2\text{Si}_2$  measured at 30 K for the momentum regions around (a)  $\Gamma(Z)$  and (b)  $X(X)$  points in the Brillouin zone. The energy dispersions of the Ru 4d bands are roughly traced with dashed lines.

here that the present interpretation method is based on the assumption of a large momentum broadening and a small transition matrix and final state effect. In this study, we have observed some indirect experimental evidences for the substantial momentum broadening perpendicular to the surface. In Fig. 3(a), we find that (1) almost of all the experimental bands are symmetric with respect to the  $X(X)$  point at the Brillouin-zone boundary and (2) the experimental band dispersions around the  $\Gamma(Z)$  point in the next Brillouin zone are almost the same as those in the first Brillouin zone. These behaviors of the experimental band dispersions are not expected if the momentum perpendicular to the surface is strictly conserved or the momentum broadening is much smaller than the size of Brillouin zone. In return, these experimental facts suggest that the above interpretation is valid for the case of  $\text{URu}_2\text{Si}_2$ . In addition, the observed bands show the periodicity matching well with the bulk Brillouin zone, which indicates that the bands are of bulk origin.

In Fig. 3(b), we show the result of the band-structure calculation<sup>16</sup> performed for the two parallel high-symmetry lines,  $\Gamma X$  (dashed lines) and  $ZR$  (solid lines). According to the calculation, the main body of the valence band consists of the Ru 4d and Si 3p states while the less dispersive bands near  $E_F$  have a strong U 5f-Ru 4d hybridized character. As found in Fig. 3, the overall feature of the valence-band structure shows a qualitatively good agreement between the experiment and the calculation. For example, we find three prominent bands from  $E_F$  to 1 eV binding energy at the  $\Gamma(Z)$  point in the experiment, which show a remarkable downward energy dispersion toward the  $X(X)$  point. By comparing the experimental band dispersions with the calculation, the two experimental bands located closer to  $E_F$  are ascribed to the highly dispersive bands on the  $ZRX$  high-symmetry line in the calculation, while the third experimental band located at 0.9 eV at the  $\Gamma(Z)$  point is assigned to a less dispersive calculated band on the  $\Gamma X$  high-symmetry line. In the higher binding energy region, we also find a good

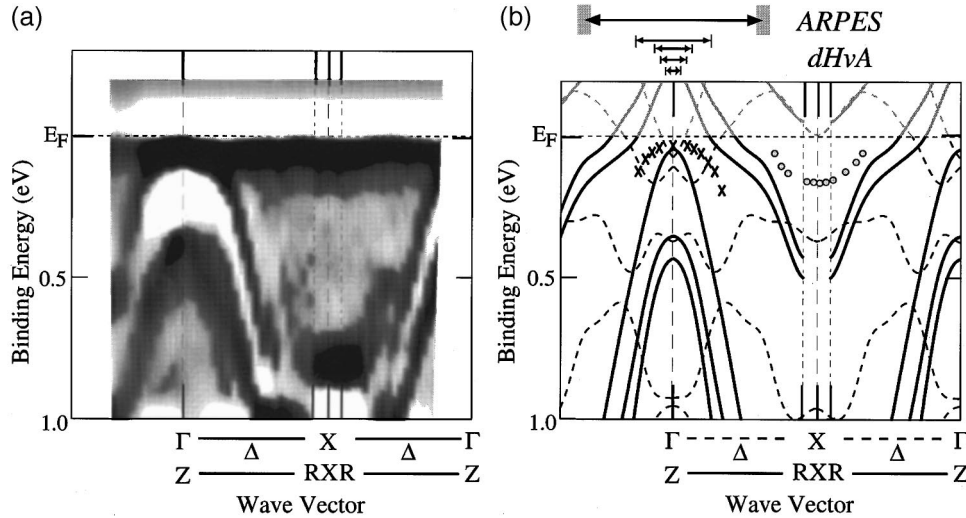


FIG. 5. Comparison of the band structure near  $E_F$  of URu<sub>2</sub>Si<sub>2</sub> between (a) the ARPES experiment and (b) the band calculation (Ref. 16). The peak positions of the topmost Ru 4*d* band and the U 5*f*-Ru 4*d* hybridized band in the ARPES spectra (Fig. 6) are superimposed in the calculation with crosses and open circles, respectively. The Fermi momenta observed by the present ARPES and the dHvA experiments (Refs. 7–9) are shown in a upper panel of the calculation. The uncertainty of the Fermi momentum by ARPES due to the finite angular resolution is shown by shading.

correspondence in the band dispersion between the experiment and the calculation, although the experimental bands become less clear owing to the intrinsic lifetime broadening at the higher binding energy. In spite of the good qualitative agreement, there are some quantitative differences between the experiment and the calculation. For example, we have not observed any bands in the energy range of 1.0–2.0 eV at the  $\Gamma(Z)$  point as shown in Fig. 3(a), while the band structure calculation predicts several bands in the same energy and momentum region. However, it is stressed here that the band-structure calculation is a good approximation to interpret the overall valence-band structure. In the energy region near  $E_F$ , on the other hand, a strong hybridization from the U 5*f* states is expected.

In Fig. 4, we show ARPES spectra near  $E_F$  measured with a smaller energy interval. Figures 4(a) and (b) correspond to the momentum regions near the  $\Gamma(Z)$  and  $X(X)$  points in the Brillouin zone, respectively. The dispersive bands marked by dashed lines in Fig. 4 correspond to the highly dispersive Ru 4*d* bands, whose dispersive feature is found to be fairly well reproduced in the band calculation as shown in Fig. 3(b). In Fig. 4(a), we find that the topmost Ru 4*d* band is situated about 30 meV away from  $E_F$  even when it approaches closest to  $E_F$  at  $\theta=0^\circ$  and thus does not seem to cross  $E_F$  as predicted by the band calculation.<sup>16</sup> In contrast to the Ru 4*d* band which disperses to the higher binding energy from the  $\Gamma(Z)$  to the  $X(X)$  point, we recognize additional broad structures just below  $E_F$ , where a substantial contribution from the U 5*f* states is expected. For example, the topmost Ru 4*d* peak has a broad shoulder at the lower-binding energy side at  $\theta=7^\circ$ – $8^\circ$ . Furthermore, around the  $X(X)$  point in Fig. 4(b), we find a broad structure in the vicinity of  $E_F$ , where several dispersive U 5*f*-Ru 4*d* hybridized bands are predicted by the band-structure calculation. Figure 5 shows comparison of the experimental band structure near  $E_F$  obtained by the ARPES with the band structure calculation.<sup>16</sup> The experimental band structure has been obtained with the same procedure as in Fig. 3. As described above, the overall feature of the Ru 4*d*

bands near the  $\Gamma(Z)$  point shows a qualitatively good agreement between the experiment and the calculation. In contrast, while the band-structure calculation predicts the comparably dispersive U 5*f*-Ru 4*d* hybridized bands near  $E_F$  around the  $X(X)$  point, the experimental band structure exhibits a broad vague structure from  $E_F$  to 200 meV binding energy in the same momentum region. This may suggest that the real U 5*f*-Ru 4*d* hybridized bands are considerably narrow and located very close to  $E_F$ .

In order to check this point, we have measured ARPES spectra near  $E_F$  in detail with a higher energy resolution and a smaller energy interval. The result is shown in Fig. 6. We again find a very sharp peak near  $E_F$  around the  $\Gamma(Z)$  point

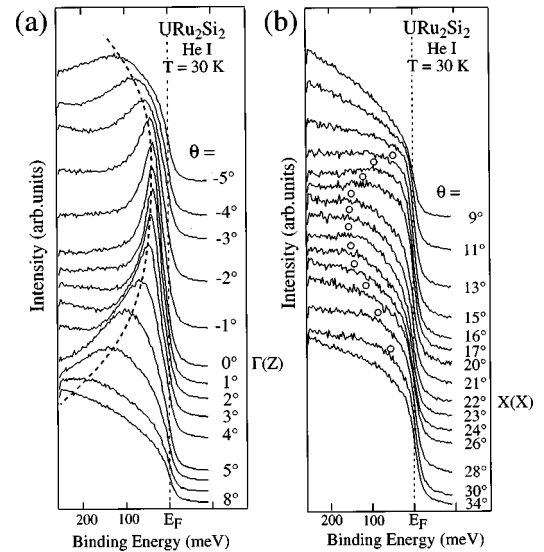


FIG. 6. ARPES spectra in the very vicinity of  $E_F$  of URu<sub>2</sub>Si<sub>2</sub> measured at 30 K for the momentum regions around (a)  $\Gamma(Z)$  and (b)  $X(X)$  points in the Brillouin zone. The energy dispersion of the U 5*f*-Ru 4*d* hybridized band around the  $X$  point is roughly traced with open circles.

[Fig. 6(a)], which has been assigned to the topmost Ru 4*d* band. It is clear in Fig. 6(a) that the  $E_F$  position is situated below the midpoint of the leading edge of ARPES spectrum near  $E_F$  even when the peak approaches closest to  $E_F$  ( $\theta = 0^\circ$ ).<sup>17</sup> This confirms that the Ru 4*d* band is totally occupied consistent with the band calculation. However, we notice that the curvature of the Ru 4*d* band near  $E_F$  around the  $\Gamma(Z)$  point is considerably flatter in the experiment than in the calculation. This indicates that the band-structure calculation underestimates the hybridization strength between the Ru 4*d* and the U 5*f* states near the  $Z$  point, suggesting that the topmost “Ru 4*d* band” has a substantial U 5*f* character near  $E_F$  through the hybridization. In fact, as found in Fig. 5(a), the experimental second Ru 4*d* band located at 0.4 eV at the  $\Gamma(Z)$  point has a sharper curvature compared with the topmost “Ru 4*d* band,” while the both have almost the same curvature in the calculation. This difference reinforces the above interpretation that the topmost “Ru 4*d* band” is flattened near  $E_F$  through the hybridization with the U 5*f* states. This suggests that the U 5*f*-Ru 4*d* hybridized bands around the  $X(X)$  point predicted from the band-structure calculation would be much flattened or narrowed because of the substantial U 5*f* character in the bands.

In the ARPES spectra near  $E_F$  around the  $X(X)$  point in Fig. 6(b), we do not find a sharp peak as observed around the  $\Gamma(Z)$  point, but instead recognize a systematic variation of the photoemission intensity near  $E_F$  with the polar angle (momentum). As found in Fig. 6(b), the intensity near  $E_F$  is considerably suppressed at  $\theta=9^\circ$  but it suddenly increases when the polar angle is increased to  $\theta=11^\circ$  and  $13^\circ$ . This suggests that a band may enter the occupied states with crossing  $E_F$  around  $\theta=11^\circ-13^\circ$ . With further increasing the polar angle, the photoemission intensity near  $E_F$  gradually increases as evident by the change of the curvature of the ARPES spectrum near  $E_F$ : we clearly find a small peak around 100 meV in the spectrum of  $\theta=16^\circ$ . We have confirmed the reproducibility of this small systematic variation of the ARPES intensity near  $E_F$  for several measurements with different samples. However, since the structure is weak and broad, the apparent position might be distorted by external effects such as a relatively large background. We have roughly traced the dispersion with open circles in Fig. 6(b). The band appears to have a bottom at about 150 meV binding energy around  $\theta=22^\circ$  and reenters the unoccupied states around  $\theta=30^\circ$ . Since the momentum of  $\theta=22^\circ$  corresponds to the  $X(X)$  point in the Brillouin zone, the band shows an energy dispersion symmetric with respect to the  $X(X)$  point. This may support the intrinsic nature of this small structure near  $E_F$ . We have superimposed the energy dispersion with open circles in Fig. 5(b) to compare with the band calculation. As is clear from the comparison, the observed band is assigned to the U 5*f*-Ru 4*d* hybridized band(s), which has a bottom at 400–500 meV at the  $X(X)$  point and forms the holelike Fermi surface(s) centered at the  $Z$  point in the calculation.<sup>16</sup> Here, we again find a considerable narrowing of the band dispersion near  $E_F$  in the experiment. This indicates that the strong-electron correlation between U 5*f* electrons causes the band narrowing through the renormalization effect, which is not included in the band calculation.

Finally we briefly comment on the Fermi surface of

URu<sub>2</sub>Si<sub>2</sub>. By following the energy dispersion of the experimental band near  $E_F$  around the  $X(X)$  point denoted by open circles in Fig. 5(b), we roughly estimate the  $E_F$ -crossing point, namely the Fermi momentum ( $k_F$ ) as  $k_F \sim 0.5 \text{ \AA}^{-1}$  from the  $Z$  point. The dHvA measurements on URu<sub>2</sub>Si<sub>2</sub> (Refs. 7–9) have observed at least four independent oscillations ascribable to the different Fermi surfaces. Since the dHvA frequency does not show a remarkable angular dependence, all of the four Fermi surfaces observed by the dHvA experiments are considered to be almost spherical. Under this assumption, we have estimated the Fermi momentum for each dHvA frequency as  $k_F \sim 0.05, 0.08, 0.09,$  and  $0.2 \text{ \AA}^{-1}$  and show the size of Fermi surfaces with arrows in the upper panel of Fig. 5(b), together with the Fermi momentum observed by the present ARPES experiment for comparison. It is noted here that only one of the four dHvA branches with the largest  $k_F$  has been observed by the three independent dHvA experiments<sup>7–9</sup> and assigned as an electronlike Fermi surfaces at the  $\Gamma$  point or a small holelike Fermi surfaces centered at the  $Z$  point<sup>9</sup> [see Fig. 5(b)]. The largest holelike Fermi surface has not been observed by the dHvA measurements. We find in Fig. 5(b) that the largest Fermi momentum observed by the dHvA experiments is smaller than that observed by the ARPES. This suggests that the present ARPES measurement has observed the largest holelike Fermi surface centered at the  $Z$  point, which has a strong U 5*f*-Ru 4*d* hybridized character. In contrast, we could not observe the Fermi surfaces with a smaller volume predicted around the  $\Gamma(Z)$  point. In order to resolve these smaller Fermi surfaces and compare in detail with the dHvA result as well as with the band-structure calculation, a precise ARPES experiment with higher energy and momentum resolutions is desired.

#### IV. CONCLUSION

We have experimentally determined the band structure of URu<sub>2</sub>Si<sub>2</sub> in the paramagnetic phase using the high-resolution angle-resolved photoemission spectroscopy, and compared the result with the band-structure calculation as well as the dHvA measurements. We found that the main body of the valence-band structure due to the Ru 4*d* and the Si 3*p* states consists of several highly dispersive bands qualitatively in good agreement with the band calculation. In the vicinity of  $E_F$ , we found a less dispersive band which crosses  $E_F$  midway between the  $Z$  and  $X$  points in the Brillouin zone. Comparing with the band calculation and the dHvA results, we found that this band is assigned to the U 5*f*-Ru 4*d* hybridized band, which forms a largest holelike Fermi surface centered at the  $Z$  point. We also found that the strong-renormalization effect due to the electron correlation of U 5*f* electrons remarkably narrows the bands near  $E_F$ .

#### ACKNOWLEDGMENT

The authors thank Professor O. Sakai and Dr. H. Yamagami for their useful discussion. H. K. thanks the Japan Society for the Promotion of Science for financial support. This work was supported by a grant from the Ministry of Education, Science, and Culture of Japan.

- <sup>1</sup>T. T. M. Palstra, A. A. Menovsky, J. van den Berg, A. J. Dirkmaat, P. H. Kes, G. J. Nieuwenhuys, and J. A. Mydosh, *Phys. Rev. Lett.* **55**, 2727 (1985).
- <sup>2</sup>M. B. Maple, J. W. Chen, Y. Dalichaouch, T. Kohara, C. Rossel, M. S. Torikachvili, M. W. McElfresh, and J. D. Thompson, *Phys. Rev. Lett.* **56**, 185 (1986).
- <sup>3</sup>W. Schlabitz, J. Baumann, B. Pollit, U. Rauchschwalbe, H. M. Mayer, U. Ahlheim, and C. D. Bredl, *Z. Phys. B* **62**, 171 (1986).
- <sup>4</sup>G. R. Stewart, *Rev. Mod. Phys.* **56**, 755 (1984).
- <sup>5</sup>R. H. Heffner and M. R. Norman, *Comments Condens. Matter Phys.* **17**, 361 (1996).
- <sup>6</sup>C. Broholm, H. Lin, P. T. Matthews, T. E. Mason, W. J. L. Buyers, M. F. Collins, A. A. Menovsky, J. A. Mydosh, and J. K. Kjems, *Phys. Rev. B* **43**, 12 809 (1991).
- <sup>7</sup>H. Ohkuni, T. Ishida, Y. Inada, Y. Haga, E. Yamamoto, Y. Ōnuki, and S. Takahashi, *J. Phys. Soc. Jpn.* **66**, 945 (1997).
- <sup>8</sup>C. Bergemann, S. R. Julian, G. J. McMullan, B. K. Howard, G. G. Lonzarich, P. Lejay, J. P. Brison, and J. Flouquet, *Physica B* **230–232**, 348 (1997).
- <sup>9</sup>N. Keller, S. A. J. Wieggers, J. A. A. J. Perenboom, A. de Visser, A. A. Menovsky, and J. J. M. Franse, *J. Magn. Magn. Mater.* **177–181**, 298 (1998).
- <sup>10</sup>F. J. Himpsel, *Adv. Phys.* **32**, 1 (1983).
- <sup>11</sup>H. Kumigashira, H.-D. Kim, A. Ashihara, A. Chainani, T. Yokoya, T. Takahashi, A. Uesawa, and T. Suzuki, *Phys. Rev. B* **56**, 13 654 (1997).
- <sup>12</sup>T. Ito, H. Kumigashira, Hyeong-Do Kim, T. Takahashi, N. Kimura, Y. Haga, E. Yamamoto, Y. Ōnuki, and H. Harima, *Phys. Rev. B* **59**, 8923 (1999).
- <sup>13</sup>H. Kumigashira, Hyeong-Do Kim, T. Ito, A. Ashihara, T. Takahashi, T. Suzuki, M. Nishimura, O. Sakai, Y. Kaneta, and H. Harima, *Phys. Rev. B* **58**, 7675 (1998).
- <sup>14</sup>T. Grandke, L. Ley, and M. Cardona, *Phys. Rev. B* **18**, 3847 (1978).
- <sup>15</sup>V. N. Strocov, H. I. Starnberg, P. O. Nilsson, H. E. Brauer, and L. J. Holleboom, *Phys. Rev. Lett.* **79**, 467 (1997).
- <sup>16</sup>G. J. Rozing, P. E. Mijnarends, and D. D. Koelling, *Phys. Rev. B* **43**, 9515 (1991).
- <sup>17</sup>We have performed numerical simulations to check the  $E_F$  crossing of the Ru 4*d* band, using parameters of a finite energy resolution and a temperature effect (Fermi-distribution function). We have calculated ARPES spectra for several cases where the Ru 4*d* band at  $\Gamma$  point is (1) 30 meV below  $E_F$ , (2) 10 meV below  $E_F$ , (3) just on  $E_F$ , and (4) 10 meV above  $E_F$ . We found that in the latter two cases, (3) and (4), the  $E_F$  position is located above the midpoint of the leading edge of ARPES spectra at  $E_F$ , while in case (1), the  $E_F$  position is situated below the midpoint. Since the present experimental result is consistent with the case (1), we have concluded that the Ru 4*d* band at  $\Gamma$  point is located below  $E_F$ .